AD_____

Award Number: W81XWH-10-2-0054

TITLE: Stem Cell Therapy for Healing Wounded Skin and Soft Tissues

PRINCIPAL INVESTIGATOR: Dr. Kai P. Leung

CONTRACTING ORGANIZATION: The Geneva Foundation
Tacoma, WA 98402

REPORT DATE: July 2011

TYPE OF REPORT: Annual

PREPARED FOR: U.S. Army Medical Research and Materiel Command
Fort Detrick, Maryland 21702-5012

REPORT DOCUMENTATION PAGE

Form Approved
OMB No. 0704-0188

1. REPORT DATE	**2. REPORT TYPE**	**3. DATES COVERED**
1 Jul 2011	Annual	15 JUN 2010 - 14 JUN 2011

4. TITLE AND SUBTITLE

Stem Cell Therapy for Healing Wounded Skin and Soft Tissues

5a. CONTRACT NUMBER

5b. GRANT NUMBER
W81XWH-10-2-0054

5c. PROGRAM ELEMENT NUMBER

6. AUTHOR(S)

Dr. Kai P. Leung

E-Mail: kai.leung@us.army.mil

5d. PROJECT NUMBER

5e. TASK NUMBER

5f. WORK UNIT NUMBER

7. PERFORMING ORGANIZATION NAME(S) AND ADDRESS(ES)

The Geneva Foundation
Tacoma, WA 98402

8. PERFORMING ORGANIZATION REPORT NUMBER

9. SPONSORING / MONITORING AGENCY NAME(S) AND ADDRESS(ES)
U.S. Army Medical Research and Materiel Command
Fort Detrick, Maryland 21702-5012

10. SPONSOR/MONITOR'S ACRONYM(S)

11. SPONSOR/MONITOR'S REPORT NUMBER(S)

12. DISTRIBUTION / AVAILABILITY STATEMENT
Approved for Public Release; Distribution Unlimited

13. SUPPLEMENTARY NOTES

14. ABSTRACT

Profiling of Paracrine Factors secreted by Leporine-deprived Mesenchymal stem cells.

15. SUBJECT TERMS
Adipose-derived Mesenchymal stem cells, cytokines, paracrine factors

16. SECURITY CLASSIFICATION OF:			**17. LIMITATION OF ABSTRACT**	**18. NUMBER OF PAGES**	**19a. NAME OF RESPONSIBLE PERSON**
a. REPORT	**b. ABSTRACT**	**c. THIS PAGE**			USAMRMC
U	U	U	UU	32	**19b. TELEPHONE NUMBER** *(include area code)*

Table of Contents

INTRODUCTION:

Exogenously applied stem cells can integrate into wounds, and if properly directed to regenerate tissue rather than to rapidly restore the barrier function, should be able to regenerate tissue for improved wound healing. We hypothesize that when applied topically to wounds, adult, adipose-derived mesenchymal stem cells that are directed toward tissue regeneration can reduce inflammation, increase angiogenesis, reduce scarring, and improve the restoration of skin functions. The goal of the proposed research is to define the function of stem cells alone or in matrix to promote healing by regeneration to improve wound repair outcomes.

BODY

I. Isolation and culture of rabbit primary cell lines.

1. Adipose derived stem cell (ASC)

ASCs were isolated from young female New Zealand White rabbits (3-4 months old, ~2.5-3.5 kg). Briefly, a ventral midline incision was made through the rabbit's dermis, and additional incisions were made from flank to flank at the rostral and caudal aspects of the midline incision. The skin was separated from the underlying adipose tissue. The inguinal fat pads were dissected out and placed in sterile, pre-warmed phosphate-buffered saline (PBS). Each fat pad yielded approximately 5-10 grams of tissue after removing evident blood vessels. Fat pads were then washed several times in PBS, minced manually, and digested in 0.075% Type II collagenase type in Hank's Buffered Salt Solution (HBSS) for 1 hour at 37°C in a shaking water bath. After digestion and inactivation of collagenase, the stromal vascular fraction (SVF) containing ASCs was isolated by centrifugation at 500 × g for 5 minutes. The SVF was resuspended in HBSS and filtered through a 100 μm sterile nylon mesh filter and then spun again at 500 × g for 5 minutes. The resultant pellet was resuspended in 10 ml of red blood cell (RBC) lysis buffer, and allowed to sit at room temperature for 10 minutes. The supernatant was removed by centrifugation following RBC lysis and the pellet was resuspened in Dulbecco's Modified Eagle Medium: Nutrient Mixture F-12 (DMEM/F12) containing 10% fetal bovine serum (FBS) and plated in 10 cm plates. After overnight culture, the media was then removed and replaced. Cells were typically confluent within 3-4 days (Figure 1A). Four primary rabbit ASC cell lines and passaged 0 to 5 (P0-P5) per each ASCs were made. The lines were stored in liquid nitrogen.

2. Dermal fibroblast (DF)

DFs were isolated from the ears of young female New Zealand White rabbits. The rabbit ear tissue was cut into squared pieces (~ 1 × 1 cm^2) and the skin tissue from the dorsal side removed. After washing with PBS, the tissue was placed with the epidermis face down in a tissue culture-grade petri dish. PBS containing Dispase at 5 mg/ml was added and incubated overnight at 4°C. Epidermal tissue was carefully excised, and

dermal tissue was minced manually and digested in 0.25% Type II collagenase in HBSS at 37°C overnight. After digestion, the solution was filtered through a 100 μm sterile nylon mesh filter and spun at 500 × g for 10 minutes. The pellet was resuspended in DMEM medium containing 10% FBS and plated in 10 cm dishes (Figure 1B). Three primary rabbit DF cell lines were made and stored in liquid nitrogen.

3. Bone marrow derived mesenchymal stem cell (BM-MSC)

BM-MSCs were isolated from the femoral medullary cavities of young female New Zealand White rabbits. Briefly, bone marrow was collected in PBS containing 2 units/ml heparin and left at room temperature for 10 minutes. After removing the floating fat layer, the solution was added to 5 ml of Ficoll-Paque Plus (1.077 g/ml, GE Healthcare, Piscataway, NJ) in a 15 ml tube and centrifuged at 2,000 × g for 30 minutes. The interface layer containing BM-MSCs was recovered and washed in HBSS. BM-MSCs were then cultured in Minimum Essential Medium (MEM) containing 10% FBS (Figure 1C). Seven primary rabbit BM-MSCs lines were made and stored in liquid nitrogen.

II. Characterization of rabbit mesenchymal stem cells

Unlike embryonic stem cells, which have specific makers such as Oct-4 and SSEA, MSCs can not be characterized by specific markers because definitive cellular markers have not yet been identified. Thus, a series of positive and negative surface markers are needed for the characterization of MSCs [1-4]. We selected CD29, CD44, CD90, and CD105 as positive markers. CD34 (endothelial cell marker) and CD45 (hematopoietic cell marker) were used as negative markers.

1. Analysis of MSC surface markers by Western blot analysis

All the antibodies that we tested were made to detect human antigens. Specificity of CD29, CD44, CD90, CD105, and CD34 were confirmed by Western blot analysis (data not shown). However, rabbit CD45 specific antibodies were not found by Western blot analysis using anti-CD45 antibodies from four different vendors (Abcam, BD Biosciences (San Jose, CA), Santa Cruz Biotechnology (Santa Cruz, CA), Thermo Scientific (Rockford, IL)). Rabbit ASCs and BM-MSCs cells [passage 1 to 9 (P1-P9)] were washed with PBS, harvested, and lysed with RIPA buffer (150 mM NaCl, 1% NP-40, 0.5% deoxycholic acid, 0.1% SDS, 50 mM Tris-Cl, pH 7.5). Equal amounts of protein were added to a 10% SDS polyacrylamide gel and trans blotted on polyvinylidene difluoride-nitrocellulose filters. Membranes were incubated with anti-CD29 (1:5,000 dilution; Abcam, Cambridge, MA), anti-CD44 (1:5,000 dilution; Abcam), anti-CD90 (1:5,000 dilution; Abcam), or anti-CD105 (1:2,500 dilution, Abcam) and then incubated with horseradish peroxide-conjugated secondary antibody (1:5,000 dilution; Vector Laboratories, Burlingame, CA). Specific bands were visualized using an Enhanced Chemiluminescence (ECL) detection kit (GE Healthcare). The blots were probed with anti-β-actin antibody (1:5,000 dilution; Sigma–Aldrich, St. Louis, MO) to serve as a control for gel loading. Expression of CD29, CD44, CD90, and CD105 were detected

without significant changes from passage 1 through passage 9 in both ASCs and BM-MSCs (Figure 2).

2. Analysis of MSC surface markers by immunofluorescence microscopy

To characterized native surface antigens without denaturing, we performed immunofluorescece microscopy on test cells. ASCs and BM-MSCs were cultured on glass cover slides, fixed in 4% paraformaldehyde, and immunostaining was performed. Fixed cells were incubated with anti-CD29 (1:200 dilution; Abcam), anti-CD44 (1:200 dilution; Abcam), anti-CD90 (1:200 dilution; Abcam), anti-CD105 (1:100 dilution, Abcam), or anti-CD34 (1:100 dilution; Abcam) as primary antibodies. Alexa Fluor 488 (Molecular Probes, Eugene, OR) conjugated secondary antibodies were used to detect specific primary antibodies. Expression of CD44 was prominent both in ASCs and BM-MSCs (Figure 3). Expression of CD29 and CD105 were detected although the signal was weak in ASCs. However, those antibodies could not detect native antigen of CD29 and CD105 in BM-MSCs. The anti-CD90 antibody did not detect rabbit CD90 antigen in either ASCs or BM-MSCs. In summary, among four antibodies used for Western blot analysis only anti-CD44 works for the detection of native form of rabbit CD44 antigen in ASCs and BM-MSCs.

3. Analysis of MSC surface markers by Flow cytometry

We attempted to characterize the population of MSCs, which have CD29, CD44, CD90, and CD105 by flow cytometry. A total of 1×10^6 ASCs (or BM-MSCs) was incubated with mousse anti-CD29 and CD90 antibodies. Flow cytometry was performed with R-Phycoerythrin (PE)-conjugated anti-mouse IgG antibody (Molecular probes) using the Flow Cytometry Core Facility at the Northwestern University. Zenon Rabbit IgG Labeling Kit (Molecular Probes) was used for anti-CD44 and CD105 antibodies, which were made in rabbit, to reduce non-specific signals for the flow cytometry. However, none of the antibodies were able to detect the presence of specific rabbit surface antigen using flow cytometry (data not shown).

4. Differentiation of rabbit MSCs

MSCs have the ability to differentiate into mesodermal cells such as adipocytes, chondrocytes, osteocytes, and myocytes in response to appropriate intrinsic or extrinsic signaling [1, 5, 6]. We wanted to address the multipotency of our rabbit ASCs and BM-MSCs and used DFs as controls as a means to determine the functionality of these isolated rabbit mesenchymal cell. This was due to the fact that while the characterization of these rabbit MSCs using surface antigens worked well using Western blot analysis, there are issues with regard to the characterization of these cells using immunofluorescence microscopy and flow cytometry.

4a. Adipogenic differentiation.

ASCs, BM-MSCs, or DFs were seeded in 24 well plate at a concentration of 2×10^4 and cultured in the Adipogenesis Differentiation Medium (Life Technologies, Carlsbad, CA). After 8 days culturing, cells were fixed in 4% paraformaldehyde and stained with Oil Red O staining. There were significant amounts of lipid droplets accumulated in the cytoplasm of both ASCs and BM-MSCs (Figures 4A & C). In contrast, fewer lipid droplets were found in the cytoplasm of DFs (Figure 4B).

4b. Osteogenic differentiation.

ASCs, BM-MSCs, or DFs were seeded in a collagen-coated (50 μg/ml) 24 well plate at a concentration of 1×10^4. The cells were cultured in the Osteogenesis Differentiation Medium (Life Technologies). Cells were fixed in 4% paraformaldehyde and Alizarin Red S staining was performed to detect the presence of accumulated calcium. Positive staining for the presence of calcium was found in ASCs and BM-MSCs but not in DFs in day 28 culture (data not shown). Both ASCs and BM-MSCs showed high accumulation of calcium at day 35 culture (Figures 5A & C). DFs also showed accumulation of calcium, but with a lesser amount as compared to that of ASCs and BM-MSC at day 35 culture (Figure 5B).

4c. Chondrogenic differentiation.

A total of 8×10^4 ASCs, BM-MSCs, or DFs in 20 μl of culture medium were plated in the middle of each well in a 24 well plate. Chondrogenesis Differentiation Medium (Life Technologies) was added to cells following 3 hour of incubation. Cells were continued to be cultured to 14 or 21 days, fixed in 4% paraformaldehyde, and stained with Alician Blue, which detect sulfated proteoglycan-rich matrix. Alician Blue Positive staining for Alician Blue positive was found in ASCs and BM-MSCs at day 14 and the intensity of the stain was increase at day 21 culture (Figure6 6A & C). Alician Blue staining positive signals were also found in DFs culture but signals were weaker as compared to ASCs and BM-MSCs (Figure 6B).

4d. Analysis of adipocytes, osteocytes, and chondrocytes lineages specific genes.

ASCs, BM-MSCs, or DFs, which were cultured in adipogenic, osteogenic, and chondrogenic medium respectively, were harvested at day 8, day 21, and day 28. Total RNA was prepared by treatment with Trizol Reagent (Sigma-Aldrich, St. Louis, MO). To make cDNA, contaminated genomic DNA during RNA preparation was removed using the Turbo DNA-free kit (Ambion, Austin, TX). cDNA was made from total RNA using superscript II (Invitrogen, Carlsbad, CA) with the use of random primers (100 ng) (Invitrogen). For quantitative analyses of the expression level of mRNAs, real-time PCR analyses using SYBR green I were performed using an ABI prism 7000 sequence detection system (Applied Biosystems, Foster City, CA). PCR primers were designed using the primer3 program (http://frodo.wi.mit.edu/). Expression of each gene was normalized to the level of glyceraldehyde-3-phosphate dehydrogenase (GAPDH) to get a

ΔCt. The $2^{-\Delta\Delta Ct}$ method was used to calculate gene expression difference between differentiated and control samples. Expression of adiponectin, osteopontin, and Col10a1 – which are specific markers of adipocytes, osteocytes, and chondrocytes, respectively – were analyzed. Expression of genes was detected by PCR with the following oligonucleotides – GAPDH (5'- AGGTCATCCACGACCACTTC -3' and 5'- GTGAGTTTCCCGTTCAGCTC -3'), adiponectin (5'- CCTGGTGAGAAGGGTGAAAA -3' and 5'- GCTGAGCGGTAGACATAGGC -3'), osteopontin (5'- AGGATGAGGACGATGACCAC -3' and 5'- CACGGCCGTCGTATATTTCT -3'), col10a1 (5'- GGAAAACAAGGGGAGAGAGG -3' and 5'- CCAGGAGCACCATATCCTGT -3').

Expression of an adipocytes specific gene, adiponectin, was increased by 35-fold and 17-fold in ASCs and BM-MSCs when cultured in adipogenic medium for 8 days (Figure 7A). However, induction of adiponectin in DFs was not found in the same culture condition. Expression of an osteocytes specific gene, osteopontin, was increased by 3.2-fold and 2.7-fold in ASCs and BM-MSCs, respectively, when cultured in the osteogenic medium for 28 days (Figure 7B). In contrast, expression of osteopontin in DFs was decreased by 0.1-fold under the same culture conditions. Expression of a chondrocytes specific gene, Col10a1, was increased by 6-fold, 12-fold, and 1,515-fold in DFs, ASCs, and BM-MSCs, respectively, when cultured in the chondrogenic medium for 21 days (Figure 7C).

III. Wound healing and hypertrophic scarring studies in the rabbit ear model

1. Animal model

Young, adult New Zealand White rabbits (3-6 months, ~2-4 kg) were acclimated to standard housing and fed ad libitum under an experimental protocol approved by the Northwestern University Animal Care and Use Committee. Rabbits were anesthetized with an intramuscular injection of ketamine (45 mg/kg) and xylazine (7 mg/kg). Four to Six wounds were created per ear. Wounds were made with a 7 mm surgical punch biopsy (Acuderm, Ft. Lauderdale, FL) down to, but not through, the cartilage. Pressure was applied to create a small nick in the cartilage for histological identification, without causing a full thickness defect in the cartilage. Tissue was then elevated in an effort to remove epidermis and dermis, but left the perichondrium intact. Wounds were covered with semi-occlusive dressings (Tegaderm^{TM}, 3M Health Care, St. Paul, MN). Elizabethan collars were applied to prevent self-inflicted trauma to wounds.

2. Wound harvesting and histological analysis

For wound healing studies, on post-operative day 7, rabbits were anesthetized by intramuscular injection of ketamine (45 mg/kg) and xylazine (7 mg/kg). Rabbits were then euthanized with the administration of 200 mg/kg intracardiac Euthasol followed by a bilateral thoracotomy (Figure 8). Ears were transected and individual wounds were isolated with a 10 mm surgical punch biopsy tool (Acuderm). Wounds were then bisected, with one half immersed immediately in 10% zinc-formalin and the other half embedded

in tissue-Tek OCT (Sakura, the Netherlands) and snap frozen for future immunohistochemical analysis. Formalin-fixed wounds were processed, embedded in paraffin blocks, and then sectioned on a microtome at a thickness of 5 μm. Sections were dried on glass slides and then stained with hematoxylin and eosin (H&E) according to standard protocols. Slide images were digitized from a Nikon Eclipse 50i light microscope and subsequently analyzed using NIS Elements BR software (Nikon, Melville, NY) for the PC (Figure 9). Epithelial gap was defined as the one-dimensional distance between the encroaching epithelial edges of the two sides on a cross section, while granulation tissue gap was defined as the distance between the new granulation tissue on either side. Values were normalized for a nick-to-nick distance of 7 mm ("adjusted gap"). Epithelial and granulation tissue areas were quantified two dimensionally by encircling the respective areas on the digitized fields. Slides were analyzed and scored in a blinded fashion. Any wounds with gross and/or histological evidence of desiccation, contamination, or physical trauma were excluded from the analysis. Results were tabulated using Microsoft Excel. In planning the experiments, an effort was also made to vary which ear received treatment (e.g., for saline vs. fibrin sealant, if saline were applied to the right ear and fibrin sealant to the left ear in the first rabbit, this pattern was reversed in the next rabbit and so on). Statistical comparisons were made with the Student's t test using a significance level of $p < 0.05$.

3. Determining optimum ASCs delivery vehicles in wound healing

Though stem cells themselves are multipotent, the interactions between stem cells and their environment are important for maintaining the proper function of stem cells, i.e., differentiation into various cell types and production of signaling molecules. Proper delivery of stem cells to the wound is critical for skin and tissue repair and regeneration. Cells in suspension have been delivered to target tissues by either direct injection or systemic circulation. Alternatively, cells have been delivered using biocompatible and biodegradable matrices which support the growth of cells.

In the first series of experiments, our objective was to determine the optimal delivery vehicles for ASCs. The delivery vehicle should not have beneficial nor adverse effects in both promoting wound healing and reducing scar formation in order to determine the true effect of ASCs in the healing process. We selected fibrin and hydrogel as delivery vehicles for our test. The rationale is that fibrin, which is a natural biopolymer of blood proteins fibrinogen and thrombin, has been used as a vehicle to deliver fibroblasts, keratinocytes, and MSCs [7-11]. Likewise, hyaluronic acid, a natural component of the extracellular matrix present in dermis and in wound environments, has also been used widely in the form of hydrogel to deliver cells such as chondrocytes, valvular interstitial cells, and MSCs [12-15].

3a. Comparison fibrin vs. saline as delivery vehicles

Aliquots of the fibrinogen and thrombin components of fibrin sealant (Haemacure Corp., Sarasota, FL or Sigma-Aldrich) were prepared at concentrations of 17.3 mg/mL and 167 U/mL, respectively. This was based on our previous work involving fibrin

sealant as a delivery vehicle for use to deliver rabbit dermal fibroblasts to rabbit ear wounds [11]. For each ear (i.e., each set of 4-6 wounds), 20 μl of fibrin sealant or 15 μl of saline was delivered. Wounds were harvested at postoperative day 7 (Figure 8) and histological differences were quantified by digitization of microscope slide images and measurement of epithelial and granulation tissue distances and areas (Figure 9). Fibrin sealant treated wounds (n=8) showed similar results in the epithelial gap (Figure 10A, 3,341 ± 445 (fibrin) vs. 2,467 ± 492 μm (saline), p =0.35), percentage healed (Figure 10B, 0.52 ± 0.06 vs. 0.65 ± 0.07%, p =0.35), granulation tissue distance (Figure 10C, 1,099 ± 122 vs. 1,368 ± 124 μm, p =0.10), and granulation tissue area (Figure 10D, 707,149 ± 132,072 vs. 806,342 ± 109,803 μm^2, p =0.41) when compared with saline treated wounds (n=7). In a separate experiment, we compared Haemacure fibrin versus Sigma-Aldrich fibrin for use as a vehicle in rabbit ear wounds. There were no significant differences in the epithelial gap, percentage healed, granulation distance, and granulation tissue areas in wounds treated with either fibrin at postoperative day 7 (data not shown).

3b. Comparison hydrogels vs. saline as delivery vehicles

Three hyaluronan based hydrogel matrices (Extracel™, Extracel-HP™, and Hystem™) were prepared according to the manufacturer's protocol (Glycogsan BioSystems, Salt Lake City, UT). The Extracel™ consists of hyaluronan (a major constituent of native ECM) and gelatin (denatured collagen). The Extracel-HP™ consists of Heprasil™ (a combination of hyaluronan and heparin) and Gelin-S™ (thiol-modified gelatin). The Hystem™ contains hyaluronan. Matrices were solidified by adding a crosslinker (polyethylene glycol diacrylate) at room temperature for 25 minutes. For each ear (i.e., each set of 4-6 wounds), 20 μl of hydrogel or 15 μl of saline was delivered to each wound. Wounds were harvested at postoperative day 7 for histological analyses. We compared between ears on the same animal to minimize the effects of rabbit-to-rabbit variation in wound healing (data not shown). For the comparison of all test vehicles at the same time, wound healing parameters of each vehicle treated sample were compared the pooled saline treated samples using the SAS ANOVA with Tukey's test (Figure 11). Hydrogel treated wounds (n=8/10/10 for Extracel, Extracel-HP, and Hystem, respectively) showed significant decrease of wound healing in the mean epithelial gap (Figure 11A, 4,599 ± 219 with p=0.0004 (Extracel), 5,159±247 with p<0.0001 (Extracel-HP), 5,374±193 with p<0.0001 (Hystem) vs. 2,384 ± 277 μm (Saline)) and percentage healed (Figure 11B, 0.34± 0.03 with p=0.0005, 0.26±0.04 with p<0.0001, 0.23±0.03 with p<0.0001 vs. 0.66 ± 0.04) when compared with saline treated wounds (n=35). There was no significant difference in saline vs. hyrodgel treated wounds for granulation tissue distance (Figure 11C, 797 ± 94 with p=0.10, 751 ± 63 with p=0.02, 828 ± 59 with p=0.10 μm vs. 1,155 ± 75 μm) and granulation tissue area (Figure 11D, 452,299±56,734 with p=0.30, 464,995 ± 74,792 with p=0.30, 693,786 ± 53,336 with p=1 vs. 723,417 ± 76,271 μm^2). Furthermore, infiltration of polymorphonuclear leukocytes (PMN) was drastically increased in hydrogel-treated wounds (data not shown).

In summary, while fibrin sealant does not affect wound healing in rabbit ear wounds, the hydrogels we tested provoked significant inflammatory reactions in host tissues.

4. Comparison of saline vs. fibrin as delivery vehicles for ASCs in wound healing

ASCs can be delivered to wounds either in suspension or in matrices. Extracellular matrices, synthetic or naturally derived, have served effectively as scaffolds for cell delivery and formation of new tissue [16, 17]. Enhanced wound healing by stem cells seeded on matrices has been reported [18, 19]. In this experiment we compared whether there is any difference in healing response between ASCs delivered in fibrin versus saline. On the day of surgery, ASCs were trypsinized from 10 cm plates, resuspended in media, and counted with the use of a hemacytometer. A total of 7×10^5 cells were harvest at 500 $\times$ g for 5 minutes, washed in PBS to remove cell culture medium, and resuspended in 70 μL of the fibrinogen component. Then, 1×10^5 cells in 10 μL of the fibrinogen were evenly placed in a 7 mm wound and 10 μL of the thrombin was applied to solidify the fibrin and ASCs mixtures. In the contralateral ear, 1×10^5 ASCs in 15 μl PBS was delivered to each wound. In addition, preparation of fibrins from different vendors was also tested. Same amounts of fibrins from Haemacure Corporation versus Sigma-Aldrich were used in the comparison. Wounds were harvested at postoperative day 7 and histological analysis was performed. As illustrated in Figure 12, Haemacure fibrin-treated wounds (n=10) showed similar results in the epithelial gap [Figure 12A, 3,788 ± 580 (Haemacure fibrin) vs. 4,408 ± 345 μm (saline), p =0.55], percentage healed (Figure 12B, 0.46 ± 0.08 vs. 0.37 ± 0.05, p =0.55), and granulation tissue distance (Figure 12C, 1,952± 393 vs. 1,941 ± 435 μm, p =0.45) when compared with saline treated wounds (n=9). More granulation tissue area was found in Haemacure fibrin- treated wounds as compared to that of saline-treated wounds (Figure 12D, 1,220,840 ± 210,981 vs. 743,558 ± 175,440 μm^2, p =0.03). In addition Sigma-Adrich fibrin-treated wounds (n=8) showed similar results as compared to Haemacure fibrin-treated wounds with regard to the epithelial gap [Figure 13A, 4,128 ± 295 (Sigma-Aldrich fibrin) vs. 3,109 ± 523 μm (saline), p =0.43], percentage healed (Figure 13B, 40.41 ± 0.04 vs. 0.56 ± 0.07, p =0.43), granulation tissue distance (Figure 13C, 41928 ± 417 vs. 1512 ± 169 μm, p =0.06), and granulation tissue area (Figure 13D, 1,091,682 ± 189,786 vs. 842,229 ± 209,110 μm^2, p =0.03).

5. *In Vitro* Optimization of Cell Seeding Density in Fibrin Gel

Rabbit ASCs (P6-P7) were harvested with trypsin-EDTA and counted. Fibrinogen-containing component of the fibrin sealant was reconstituted and diluted using Tris-buffered saline (TBS) to yield a working stock solution of 17.3mg/mL. Three concentrations of ASCs (10,000 cells/μL, 1,000 cells/μL, 100 cells/μL) were resuspended in fibrinogen and added to a flat bottom 96-well plate (TPP, dia=6.7mm). Equal volumes of thrombin (167 U/mL) were added to each well and the fibrin mixture was allowed to

further solidify at 37°C for 30min before serum-containing plating media was added to each well.

The MTT assay (Molecular Probes) was used to determine cell viability and cell proliferation of rabbit ASCs in the fibrin sealant. Briefly, a stock solution of 3-(4,5-Dimethylthiazol-2-y)-2,5-diphenyltetrazolium bromide (MTT) was prepared at a concentration of 5 mg/mL. Ten μL of this solution was added to each well containing 100 μL of phenol red free DMEM/F12 + 10% serum, and incubated at 37°C and 5% CO_2 for 4 hr. After complete removal of the media/MTT solution, 200 μL of isopropanol-acetone (IPA) mixture (1:3) was added to each well and incubated for 1hr. The absorbance of each of the wells was measured at 570 nm using a spectrophotometer. Cell proliferation of rabbit ASCs over the course of 7 days is shown in Figure 14 with three different initial seeding densities. At 1,000 cells/μL or 100 cells/μL, ASCs proliferated well, whereas at 10,000 cells/μL, a reduction in cell proliferation was seen over time.

The Live/Dead Viability/Cytotoxicity Assay (Molecular Probes) was also used to provide a visualization of live and dead cells within the fibrin gel at different time points. The assay is based on the detection of two fluorescent probes (calcein AM for live cells and EthD-1 for dead cells). Briefly, the dye reagents were prepared by adding 5 μL EthD-1 (2mM stock) and 1.25 μL Calcein AM (40mM stock) to 10 mL of 1xPBS. Two hundred μL of the dye solution was added to each well, and incubated at RT for 30 min. The dye was removed promptly at the end of incubation and replaced with 200 μL of PBS/well. The wells were imaged immediately with a fluorescent/confocal microscope. Representative images are shown in Figure 15. The results indicated that there was a loss of viability for ASCs seeding in high density in fibrin gel over time.

6. Survival of delivered ASCs in wounds

ASCs can contribute to wound healing by either cytokine expression or differentiation and repopulation in wounds. It has been thought that conventional infusion of stem cells by injection has limitations such as poor delivery, retention of cells, and cell death because of loss of anchorage. Our data showed that both saline and fibrin delivered ASCs have similar results in keratinocytes migration determined by epithelial gap (Figure 12 & 13). However, higher granulation tissue area was found in wounds where ASCs were delivered in a fibrin vehicle as compared to that of ASCs delivered in saline vehicle. We wanted to determine the survivability of transplanted ASCs in wound using GFP-labeled ASCs (Figure 16). A total of 1×10^5 ASCs per wounds were delivered as described above with fibrin vehicle in one ear and saline vehicle in the contralateral ear. Wounds were harvested at postoperative day 7 and histological analysis was performed. Five μm thick sections of wounds were deparaffinized in xylene followed by graded alcohols to water and treated with antigen retrieval solution for 20 minutes in a steamer. Endogenous peroxidase activity was blocked with 3% H_2O_2 for 10 minutes. Mouse anti-GFP (1: 1,000 dilution, Sigma-Aldrich) was used as the primary antibody. Signals were detected using the Vectastain kit (Vector laboratories, Burlingame, CA) and visualized using 3,3'-diaminobenzidine (DAB). As illustrated in Figure 16, GFP signal was found in the transplanted wounds where ASCs were delivered either by saline (Figures 16 A, B,

and C) or fibrin (Figures 16A', B', and C'). In order to draw a conclusion, more wound samples are needed for the statistical analysis of survival or proliferation ratio of ASCs delivered with vehicles, fibrin vs. saline, in wounds at postoperative day 7.

In summary, ASCs both in saline and in fibrin were survived in wounds 7 days after transplantation. Though more granulation areas were found in fibrin treated wounds, there were not significant differences in epithelialization, which is the most important parameter in wound healing, between fibrin vs. saline carried ASCs. Several potential problems might be found in fibrin as a ASCs delivery vehicle in rabbit wounds; 1) fibrinogen and thrombin are human origin, which may evoke inflammation, 2) purify and quality of fibrinogen and thrombin will not be same among vendors, 3) though we used conditions based on our previous publication [11], in which fibroblasts were used, optimum condition of fibrinogen and thrombin for ASCs can be different. Thus, we will use saline as a vehicle of ASCs in wound healing study.

7. Determining the optimal delivery vehicle for ASCs and their survival in hypertrophic scar

1×10^5 ASCs was delivered in either the fibrin vehicle (Haemacure Corporation or Sigma-Aldrich) or saline to each ear wound. Wounds in one of the ear in the animal would receive ASCs in fibrin whereas a similar amount of cells in saline was given to each wound of the contralateral ear. A total of 2 rabbits were used in this preliminary study. In order to observe the effects of treatment to scar, wounds are observed over a 28-day period. The experiment was initiated in the middle of June. Wounds from two animals will be harvested at postoperative day 28 when hypertrophic scar is matured. The scar elevation index (SEI) will be measured to quantify the formation of hypertrophic scar. The SEI is a ratio of total scar area [area of newly formed dermis (neodermis) to the estimated area of unwounded dermis (non-scarred dermis)]. An SEI of 1 indicates that the wound healed essentially flat, with no scar hypertrophy and an SEI greater than 1 represents a raised, hypertrophic scar. An increasing magnitude in the SEI correlates with increasing scar prominence over the level of unwounded tissue. Wounds from two animals will be harvested in the middle of July 2011. In addition, to examine the effect of fibrin vehicle alone in the formation of scarring, fibrin or saline was treated without ASCs in wounds of rabbit ears. Wounds from two rabbits will be harvested at postoperative day 28 (middle of July 2011) and analyzed. ASCs can contribute to reducing hypertrophic scarring formation by either cytokine expression or differentiation and repopulation in wounds. Therefore, it is important to determine the survivability of ASCs in wounds over the course of 28 days. A preliminary experiment was initiated in the middle of June. A total of 1×10^5 GFP expressing ASCs per wounds were delivered as described above with fibrin vehicle in one ear and with saline vehicle in the contralateral ear of one rabbit. Wounds will be harvested and expression of GFP will be analyzed.

IV. Construction and optimization of materials for animal experiments

1. Construction of living color protein expressing rabbit cells

ASCs, DFs, or rabbit dermal fibroblast cell line (CRL1414, ATCC) were labeled with green fluorescence protein (GFP) or red fluorescent protein (DsRed2) to determine the survival rate and fate of cells which are delivered in wounds. To stably express GFP (or DsRed2), ASCs were transduced with a lentivirus (LV-GFP or LV-DsRed2) in which GFP (or DsRed2) expression is driven by a cytomegalovirus (CMV) promoter (Figure 16). Briefly, 2 multiplicity of infection (MOI) of lentivirus was infected to cells in the presence of 6 μg/ml of polybrene. Transduced cells were selected by treating 10 μg/ml of blasticidin. We observed some ASCs which do not express GFP, though they grew in the presence of blasticidin (Figure 17). Thus, living color expressing cells were further selected by flow cytometry.

2. Construction of firefly luciferase (Fluc) expressing rabbit ASCs

To study topological distribution and quantitative analysis of delivered ASCs survival, Fluc was stably expressed in ASCs using lentivirus as described above (LV-Fluc, Figure 16). We used a bicistronic lentiviral vector (pLVX-IRES-ZsGreen1, Clontech, Mountain View, CA) in which Fluc and ZsGreen1 is expressed by CMV promoter and internal ribosome entry site (IRES), respectively (Figure 18). ASCs were infected with the lentivirus and ZsGreen1 expressing cells were selected by flow cytometry.

3. Optimization of immunohistochemical conditions for the study of molecular mechanism of wound healing and hypertrophic scar by MSCs treatment

The rabbit ear hypertrophic scar model has a number of parameters which behave in a similar fashion to that of human hypertrophic scar [20-24]. The model has the advantage of easy quantification of epithelialization and granulation tissue formation. In addition, the ability to create large numbers of wounds and relatively short time points for evaluation of hypertrophic scar (28-35 days) is a unique advantage of the rabbit ear model. This facilitates the determination of the role of stem cell therapy in acute and scarring wounds using the same animal model but by evaluating the wounds at different time points.

The disadvantages of working with rabbits are the lack of available published gene sequences, antibodies, and other probes as compared to rats and mice. However, the Broad Institute has completed a deep coverage (7x) draft of the rabbit genome (*Oryctolagus cuniculus*, OryCun2.0, released August, 2009). Annotation of OryCun2.0 by the National Center for Biotechnology Information (NCBI) is available in Map Viewer. It has been suggested that MSCs suppress immune reactions and have reduced histocompatability antigens. In addition, allogeneic and xenogeneic therapeutics have been considered because they have reduced expression of histocompatibility antigens and secrete immunoregulatory molecules [25-29]. At present, inflammatory reactions induced

by exogenous MSCs in transplanted host has not been well characterized yet. We have optimized the immunohistochemistry conditions to detect for the presence of neutrophils (Figure 19A) and macrophages (Figure 19D) in rabbits in order to study the potential immune reactions to transplanted MSCs in rabbit ear wounds. MSCs can contribute to wound healing and hypertrophic scarring by either cytokine expression or differentiation to specific cells in wounds. We detected GFP signals after 7 days transplantation of ASCs in wounds. However, non-proliferating ASCs might still have GFP positive signal because GFP is stable and exhibits a long half life. To address proliferation of transplanted MSCs in wound, we have optimized the immunohistochemistry conditions for the detection of Ki67 (Figure 19B) in rabbits. In addition, detection of an endothelial marker, CD31, has also been optimized (Figure 19C).

V. Cytokine Expression Profile of Rabbit and Human MSCs

The cytokine secretion profile of rabbit and human MSCs was examined by analyzing conditioned media (CM) samples collected from each cell type via enzyme-linked immunosorbent assay (ELISA). CM was prepared by incubating cells for up to 72hr in culture. Since there is a shortage of rabbit specific reagents, we resorted to commercially available human ELISA kits (R&D Systems, RayBiotech, Millipore) to measure the secretion of factors that have high percentage of homology between human and rabbit.

Under basal conditions, the expression of Transforming Growth Factor (TGF)-β1 was similar among rabbit ASCs and BMSCs, whereas the expression was significantly lower in DFs. No significant differences in the expression of TGF-β2 were found. Furthermore, TGF-β3 was not detected in both rabbit and human MSCs. Vascular Endothelial Growth Factor (VEGF) was detected in rabbit and human ASCs, BMSCs, and DFs cultured under normal conditions. The expression of VEGF was up-regulated in cells cultured in hypoxic conditions (1% O_2) (data not shown).

Current and future efforts will include analysis of other angiogenic and pro-inflammatory factors such as HGF, bFGF, IL-6 and TNF-α. Table 1 is a summary of our current findings and future efforts.

Table 1. Cytokine Expression Profile of Rabbit and Human MSCs

Cytokines*	Rb ASC[1]	Rb BMSC[2]	Rb DF[3]	hASC[4]	hBMSC[5]	hDF[6]
TGF-β_1	++	++	+[§]	++	++	+
TGF-β_2	+	+	+	+	+	+
TGF-β_3	-	-	-	-	-	-
VEGF	+	+	+	+	+	+
bFGF[¥]	TBD[€]	TBD	TBD	TBD	TBD	TBD
HGF[¥]	TBD	TBD	TBD	TBD	TBD	TBD
EGF[¥]	TBD	TBD	TBD	TBD	TBD	TBD
IL-6[¥]	TBD	TBD	TBD	TBD	TBD	TBD
TNF-α[¥]	TBD	TBD	TBD	TBD	TBD	TBD

* Conditioned media were collected from cultured cells after 72 hour of incubation at 37°C in 5% CO_2.
1: Rabbit adipose-derived mesenchymal stem cell; 2: Rabbit bone marrow-derived mesenchymal stem cell; 3: Rabbit dermal fibroblast; 4: Human adipose-derived mesenchymal stem cell; 5: Human bone marrow-derived mesenchymal stem cell; 6: Human dermal fibroblast.
§ +: presence of test cytokines.
¥ bFGF: Basic Fibroblast Growth Factor; HGF:Hepatocyte Growth Factor; EGF: Epidermal Growth Factor; IL-6: Interleukin-6; TNF-α:Tumor Necrosis Factor- α.
€ TBD: To Be Determined.

KEY RESEARCH ACCOMPLISHMENTS:

- Isolated and characterized four rabbit ASCs lines.
- Isolated and characterized eight rabbit BM-MSCs lines.
- Isolated and characterized three rabbit DFs lines.
- Established GFP (or DsRed2) expressing ASCs and DFs to study the fate of transplanted ASCs in wounds.
- Established firefly luciferase expressing ASCs.
- Optimized immunohistochemistry condition for rabbit neutrophils, macrophages, CD31, and Ki67.
- Determined saline as a MSCs delivery vehicle.
- Characterized survival of ASCs in wounds after 7 days transplantation.
- Started to perform hypertrophic scarring animal experiments.
- Rabbit and human MSC were able to secret higher levels of TGF-β1 as compared to that of fibroblasts.

REPORTABLE OUTCOMES:

Abstracts:

Lee WC, SK Hong, TA Mustoe, RG Hale, Leung KP. Profiling of Paracrine Factors Secreted by Leporine-derived Mesenchymal Stem Cells. Accepted. Advance Technology Application in combat Casualty Care. August 15- 18, Ft. Lauderdale, FL.

Primary Cell lines:

- Rabbit adipose-derived mesenchymal stem cells
- Rabbit bone marrow-derived mesenchymal stem cells
- Rabbit dermal fibroblasts
- Rabbit (ear) keratinocytes
- Rabbit (vagina) keratinocytes

CONCLUSION:

In the first year of this 2-year study, we have built most of the needed tools in order to to determine the effect of adipose-derived mesencyhmal stem cells (ASCs) for improving wound healing and scarring. These include the isolation and characterization of ACSs and other rabbit mesenchymal stem cells for their surface antigen phenotypes and ability to differentiate into adiopogenic, chondrogenic, and osteogenic lineages. Molecular tools such as GFP- or DsRed2- labeled ASCs were constructed to facilitate the study of the fate of transplanted ASCs into wounds. We have also established the rabbit hypertrophic scar model for determining the effect of transplanted stem cells on wound healing and scar compliance. We demonstrated that rabbit and human MSCs were able to secret higher levels of TGF-β1 as compared to that of fibroblasts in our profiling experiment for the paracrine factors secreted by stem cells in basal conditions (unstimulated). As a result of these experiments, we have gained knowledge with regard to the physiology of rabbit adipose-derived stem cells. We are poised to begin the hypertrophic scarring animal experiments.

In our preliminary animal work with the allogeneic ACSs transplantation to wounds, some levels of inflammatory response were observed. This could present a barrier for the use of allogeneic ASCs in our wound healing and anti-scarring experiments. Should this problem persist, we will adopt the use of autologous ASCs instead.

For impact, we are one of the very few groups to be able to isolate and characterize the rabbit ASCs for use in wound healing and reduce scarring using a clinically relevant hypertrophic scar animal model. The results of the paracrine profiling study also provide important information with regard to the mechanistic basis of stem cell activity in regenerative repair of wounds.

REFERENCES:

[1] J.M. Gimble, A.J. Katz, B.A. Bunnell, Adipose-derived stem cells for regenerative medicine, Circulation Research 100 (2007) 1249-1260.

[2] A. Schaffler, C. Buchler, Concise review: adipose tissue-derived stromal cells--basic and clinical implications for novel cell-based therapies, Stem Cells 25 (2007) 818-827.

[3] B. Lindroos, R. Suuronen, S. Miettinen, The potential of adipose stem cells in regenerative medicine, Stem Cell Rev 7 (2011) 269-291.

[4] C.S. Lin, Z.C. Xin, C.H. Deng, H. Ning, G. Lin, T.F. Lue, Defining adipose tissue-derived stem cells in tissue and in culture, Histol Histopathol 25 (2010) 807-815.

[5] B.A. Bunnell, B.T. Estes, F. Guilak, J.M. Gimble, Differentiation of adipose stem cells, Methods Mol Biol 456 (2008) 155-171.

[6] C.T. Gomillion, K.J. Burg, Stem cells and adipose tissue engineering, Biomaterials 27 (2006) 6052-6063.

[7] E. Mansilla, G.H. Marin, F. Sturla, H.E. Drago, M.A. Gil, E. Salas, M.C. Gardiner, G. Piccinelli, S. Bossi, E. Salas, L. Petrelli, G. Iorio, C.A. Ramos, C. Soratti, Human mesenchymal stem cells are tolerized by mice and improve skin and spinal cord injuries, Transplant Proc 37 (2005) 292-294.

[8] L.J. Currie, J.R. Sharpe, R. Martin, The use of fibrin glue in skin grafts and tissue-engineered skin replacements: a review, Plast Reconstr Surg 108 (2001) 1713-1726.

[9] S.J. Gwak, S.S. Kim, K. Sung, J. Han, C.Y. Choi, B.S. Kim, Synergistic effect of keratinocyte transplantation and epidermal growth factor delivery on epidermal regeneration, Cell Transplant 14 (2005) 809-817.

[10] W. Ho, B. Tawil, J.C. Dunn, B.M. Wu, The behavior of human mesenchymal stem cells in 3D fibrin clots: dependence on fibrinogen concentration and clot structure, Tissue Eng 12 (2006) 1587-1595.

[11] J. Mogford, B. Tawill, X. Jia, T. Mustoe, Fibrin sealant combined with fibroblast and platelet-derived growth factor enhance wound haealing in excisional wounds, Wound Rep Reg 17 (2009) 405-410.

[12] C.H. Jang, H. Park, Y.B. Cho, C.H. Song, Mastoid obliteration using a hyaluronic acid gel to deliver a mesenchymal stem cells-loaded demineralized bone matrix: an experimental study, Int J Pediatr Otorhinolaryngol 72 (2008) 1627-1632.

[13] G.D. Prestwich, J.W. Kuo, Chemically-modified HA for therapy and regenerative medicine, Curr Pharm Biotechnol 9 (2008) 242-245.

[14] D.N. Shah, S.M. Recktenwall-Work, K.S. Anseth, The effect of bioactive hydrogels on the secretion of extracellular matrix molecules by valvular interstitial cells, Biomaterials 29 (2008) 2060-2072.

[15] D.M. Yoon, S. Curtis, A.H. Reddi, J.P. Fisher, Addition of Hyaluronic Acid to Alginate Embedded Chondrocytes Interferes with IGF-1 Signaling In Vitro and In Vivo, Tissue Eng Part A (2009).

[16] G.C. Gurtner, S. Werner, Y. Barrandon, M.T. Longaker, Wound repair and regeneration, Nature 453 (2008) 314-321.

[17] D.E. Discher, D.J. Mooney, P.W. Zandstra, Growth factors, matrices, and forces combine and control stem cells, Science 324 (2009) 1673-1677.
[18] A.M. Altman, N. Matthias, Y. Yan, Y.H. Song, X. Bai, E.S. Chiu, D.P. Slakey, E.U. Alt, Dermal matrix as a carrier for in vivo delivery of human adipose-derived stem cells, Biomaterials 29 (2008) 1431-1442.
[19] A.M. Altman, Y. Yan, N. Matthias, X. Bai, C. Rios, A.B. Mathur, Y.H. Song, E.U. Alt, IFATS collection: Human adipose-derived stem cells seeded on a silk fibroin-chitosan scaffold enhance wound repair in a murine soft tissue injury model, Stem Cells 27 (2009) 250-258.
[20] D.E. Morris, L. Wu, L.L. Zhao, L. Bolton, S.I. Roth, D.A. Ladin, T.A. Mustoe, Acute and chronic animal models for excessive dermal scarring: quantitative studies, Plast Reconstr Surg 100 (1997) 674-681.
[21] O. Kloeters, A. Tandara, T.A. Mustoe, Hypertrophic scar model in the rabbit ear: a reproducible model for studying scar tissue behavior with new observations on silicone gel sheeting for scar reduction, Wound Repair Regen 15 Suppl 1 (2007) S40-45.
[22] J.R. Marcus, J.W. Tyrone, S. Bonomo, Y. Xia, T.A. Mustoe, Cellular mechanisms for diminished scarring with aging, Plast Reconstr Surg 105 (2000) 1591-1599.
[23] A.S. Saulis, J.D. Chao, A. Telser, J.E. Mogford, T.A. Mustoe, Silicone occlusive treatment of hypertrophic scar in the rabbit model, Aesthet Surg J 22 (2002) 147-153.
[24] L. Lu, A.S. Saulis, W.R. Liu, N.K. Roy, J.D. Chao, S. Ledbetter, T.A. Mustoe, The temporal effects of anti-TGF-beta1, 2, and 3 monoclonal antibody on wound healing and hypertrophic scar formation, J Am Coll Surg 201 (2005) 391-397.
[25] A. Uccelli, L. Moretta, V. Pistoia, Mesenchymal stem cells in health and disease, Nat Rev Immunol 8 (2008) 726-736.
[26] A.I. Caplan, Why are MSCs therapeutic? New data: new insight, J Pathol 217 (2009) 318-324.
[27] A. Bartholomew, C. Sturgeon, M. Siatskas, K. Ferrer, K. McIntosh, S. Patil, W. Hardy, S. Devine, D. Ucker, R. Deans, A. Moseley, R. Hoffman, Mesenchymal stem cells suppress lymphocyte proliferation in vitro and prolong skin graft survival in vivo, Exp Hematol 30 (2002) 42-48.
[28] K. McIntosh, S. Zvonic, S. Garrett, J.B. Mitchell, Z.E. Floyd, L. Hammill, A. Kloster, Y. Di Halvorsen, J.P. Ting, R.W. Storms, B. Goh, G. Kilroy, X. Wu, J.M. Gimble, The immunogenicity of human adipose-derived cells: temporal changes in vitro, Stem Cells 24 (2006) 1246-1253.
[29] B. Puissant, C. Barreau, P. Bourin, C. Clavel, J. Corre, C. Bousquet, C. Taureau, B. Cousin, M. Abbal, P. Laharrague, L. Penicaud, L. Casteilla, A. Blancher, Immunomodulatory effect of human adipose tissue-derived adult stem cells: comparison with bone marrow mesenchymal stem cells, Br J Haematol 129 (2005) 118-129.

APPENDICES:

None

APPENDICES:

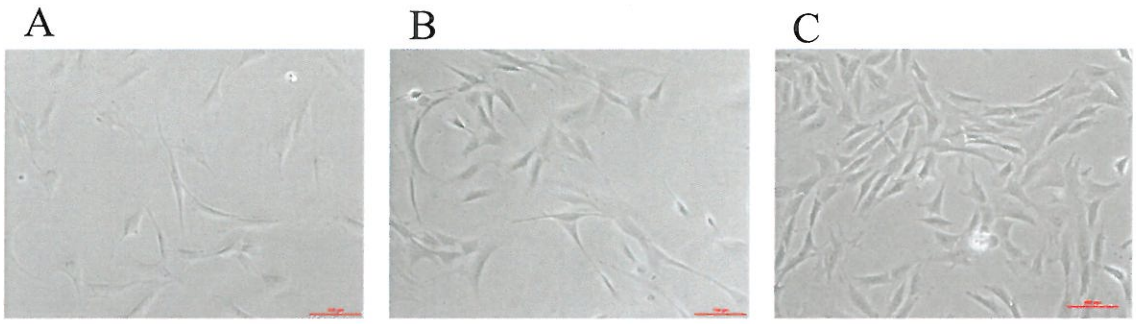

Figure 1. Morphology of rabbit adipose derived stem cells (A), dermal fibroblasts (B), and bone marrow-derived mesenchymal stem cells (C). Cells were grown in culture dishes with growth medium. Scale bar; 100 μm.

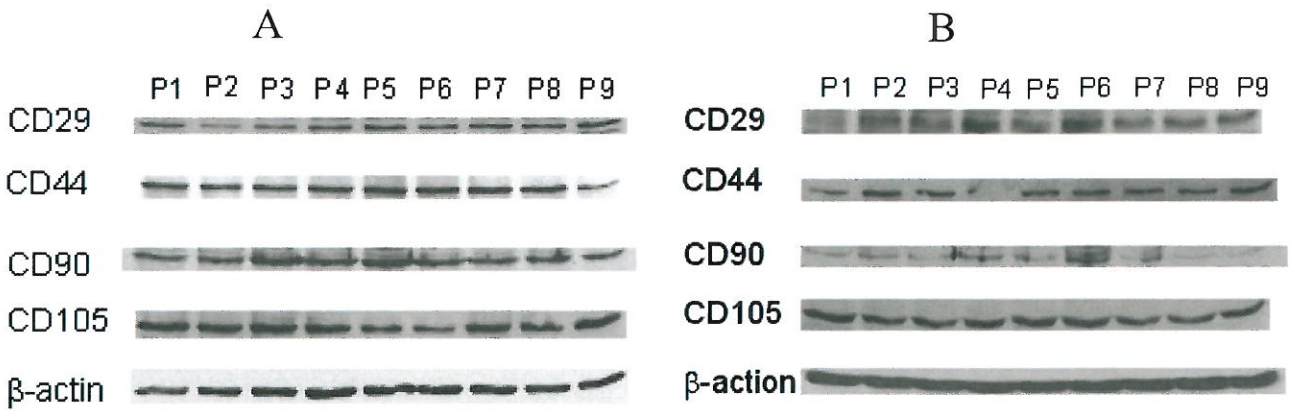

Figure 2. Expression analysis of surface markers. Rabbit ASCs (A) and BM-MSC (B) were harvested and Western blot analyses were performed. The expression of CD29, CD44, CD90, and CD105 were detected with their specific antibodies as indicated. β-actin was detected as a loading control.

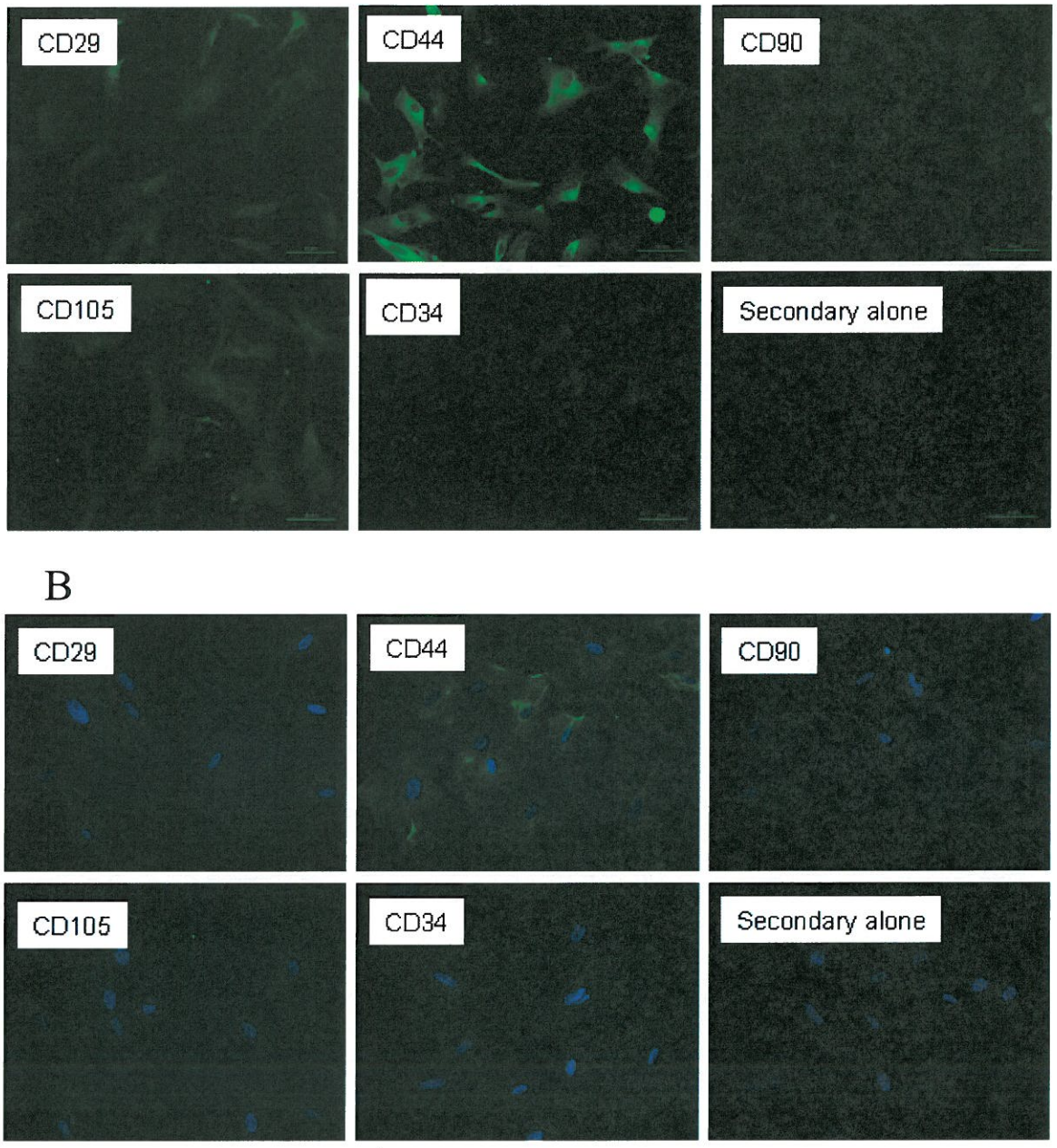

Figure 3. Expression analysis of surface markers. Rabbit ASCs at passage 1 (A) and BM-MSC at passage 2 (B) were cultured *in vitro* and immunostaining was performed. The expression of CD29, CD44, CD90, CD105, and CD44 were detected with their specific antibodies as indicated and Alexa Fluor 488 conjugated secondary antibodies were used to visualized the signal. Nuclei were stained with DAPI in B. Signals were captured with the same exposure time in each panel.

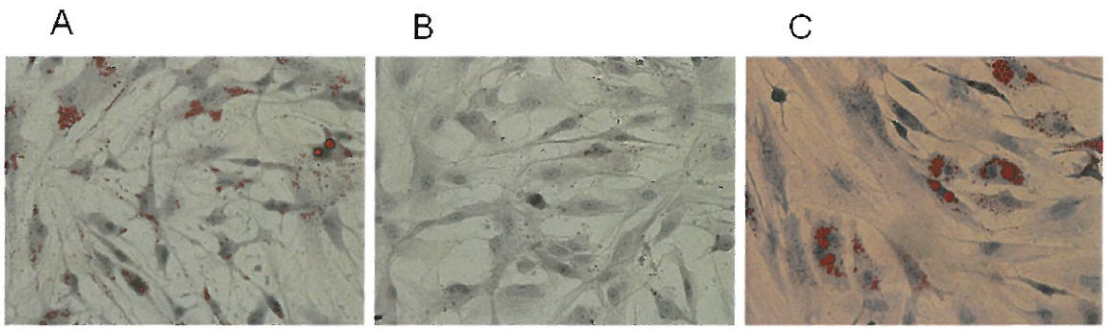

Figure 4. Adipogenic differentiation of MSCs. Rabbit ASCs (A), DFs (B), and BM-MSC (C) were cultured in adipogenesis differentiation medium for 8 days. Oil Red O staining was performed to detect lipid accumulation. Nuclei were stained with Hematoxylin.

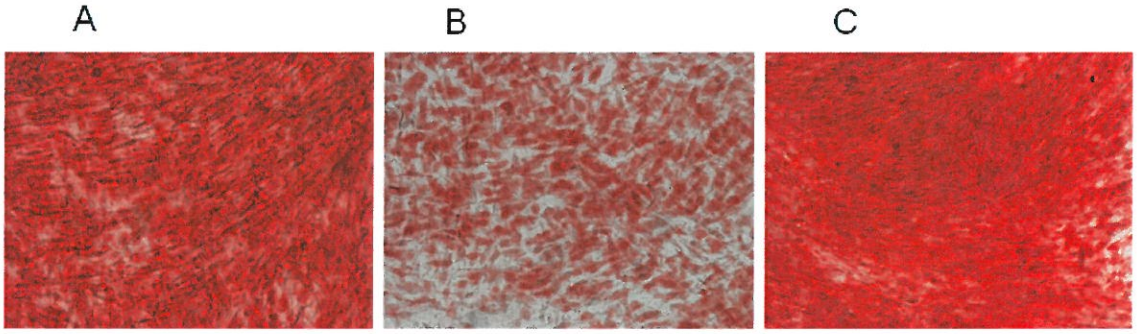

Figure 5. Osteogenic differentiation of MSCs. Rabbit ASCs (A), DFs (B), and BM-MSC (C) were cultured in osteogenesis differentiation medium for 35 days. Alizarin Red S staining was performed to detect calcium accumulation.

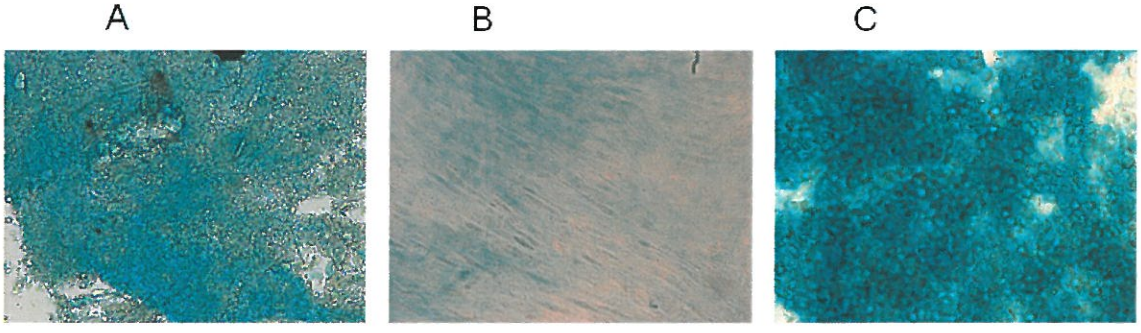

Figure 6. Chondrogenic differentiation of MSCs. Rabbit ASCs (A), DFs (B), and BM-MSC (C) were cultured in chondrogenesis differentiation medium for 21 days. Alician Blue staining was performed.

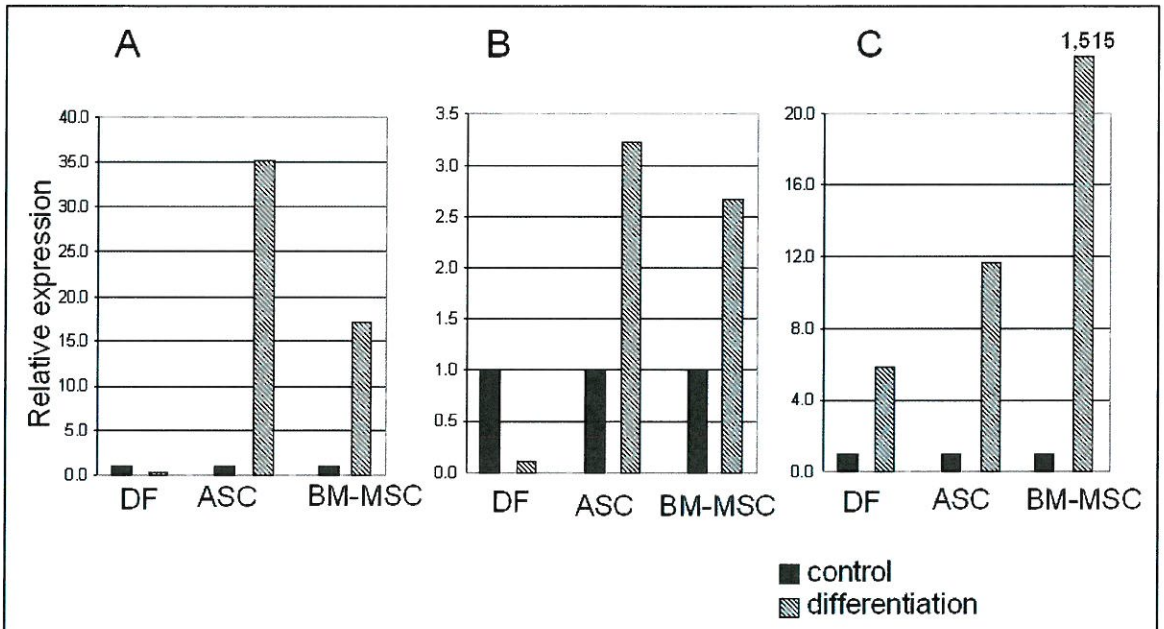

Figure 7. mRNA level of lineage specific genes was increased by differentiation. DFs, ASCs, and BM-MSCs were grown in adipogenic (A), osteogenic (B), or chondrogenic (C) medium for 8, 28, or 21 days. Total RNAs were isolated and quantitative real-time PCR was performed. Expression of adiponectin (A), osteopontin (B), and Col10a1 (C) was analyzed. Each gene expression was normalized according to the expression level of GAPDH. The level of gene expression in cells cultured in differentiation medium was compared to cells in cultured non-differentiated medium, which was set at 1.

Figure 8. A photograph of rabbit ear wounds at harvest. Fibrin sealant or saline was applied to 7 mm wounds in ear on the day of surgery (postoperative day 0). Wounds were harvested at postoperative day 7.

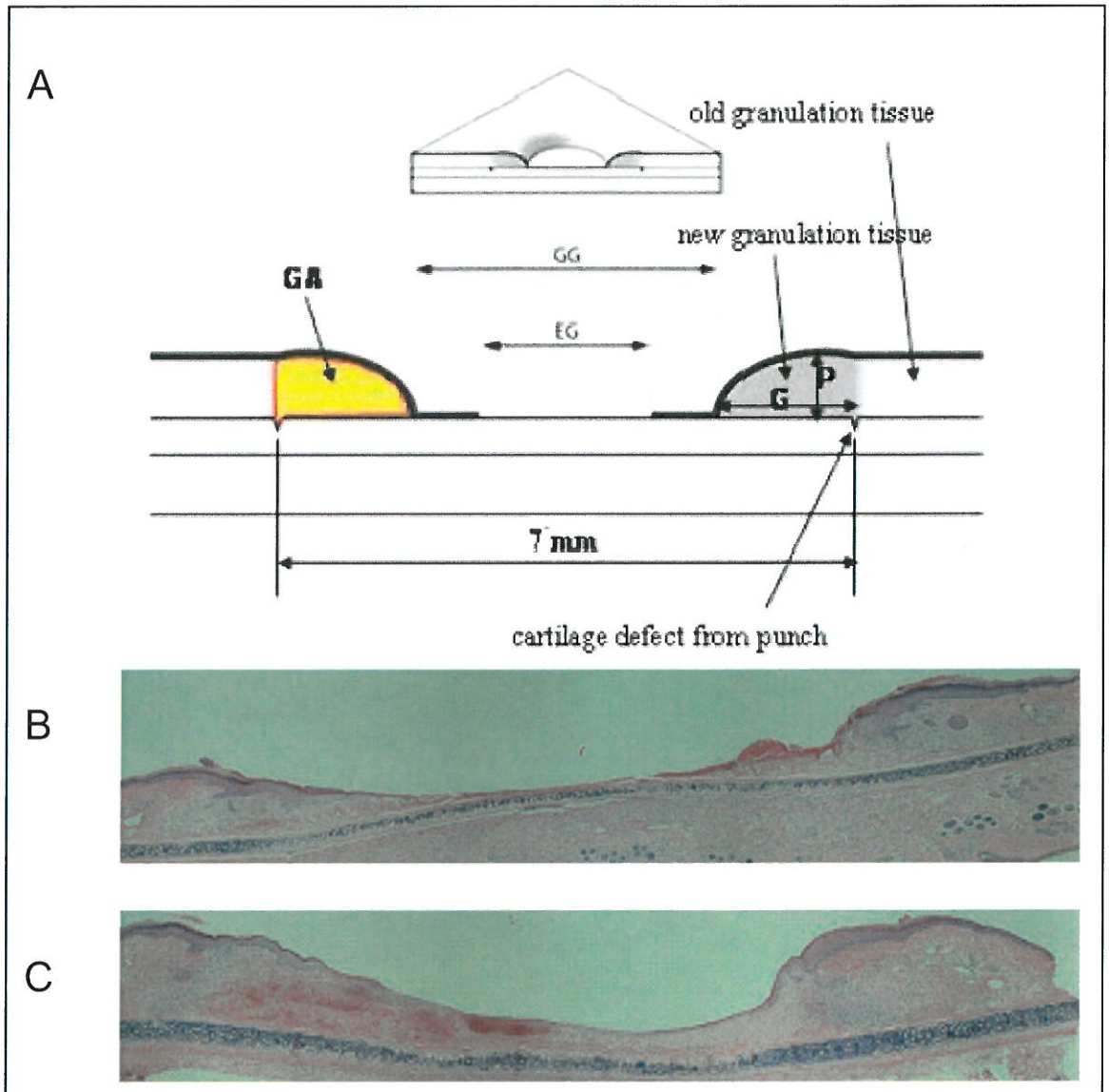

Figure 9. Schematic drawing of histological analysis. (A) EG, epithelial gap; GG, granulation gap; G, new granulation tissue distance; P, height of granulation tissue; GA, granulation area. (B, C) H&E staining of rabbit wounds 7 days after ASCs treatment either in saline (B) or in fibrin (C).

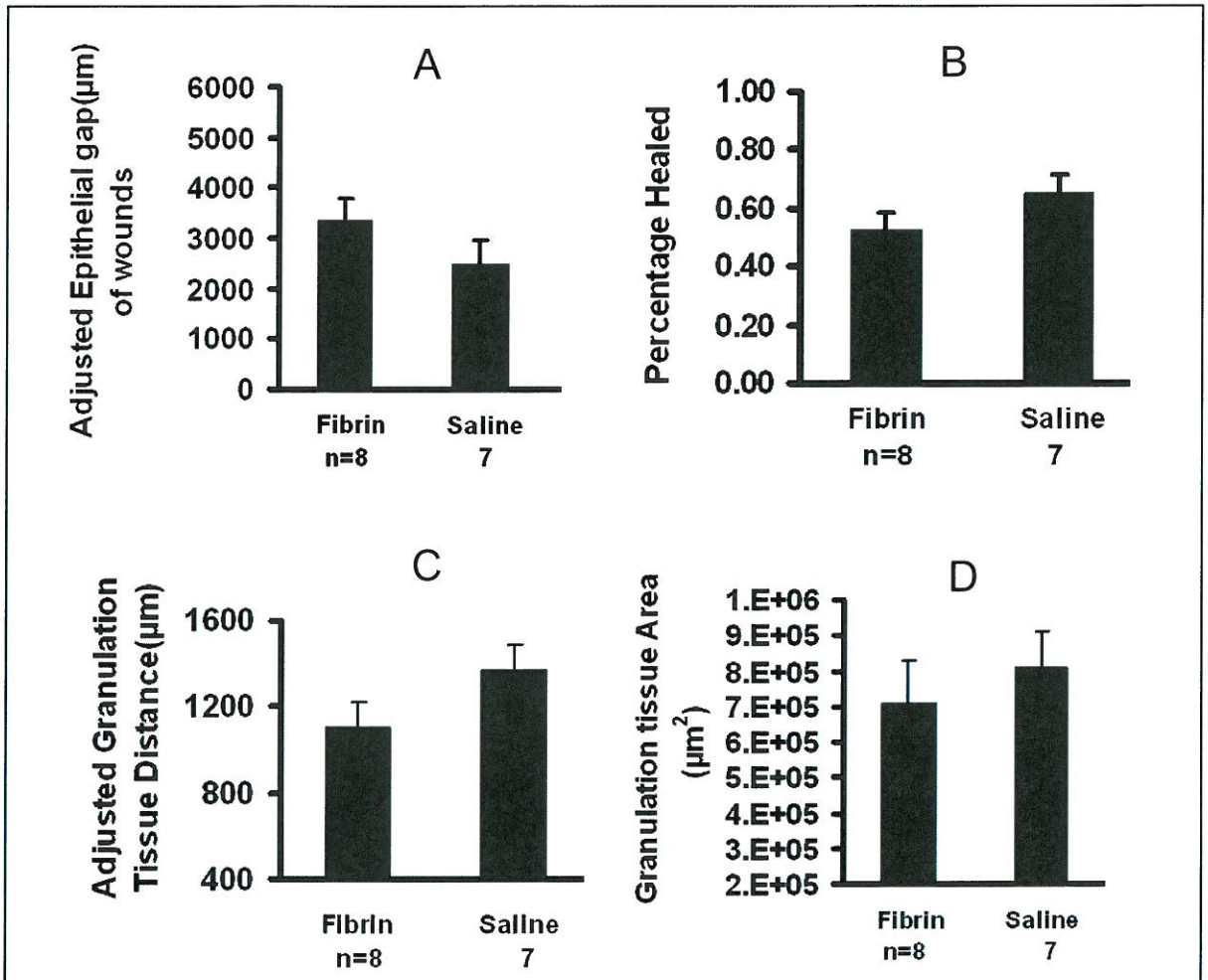

Figure 10. Histological quantification of fibrin vs. saline treated wounds. Wounds (7 mm) were analyzed for adjusted epithelial gap (A), percentage healed (B), adjusted granulation tissue distance (C), and granulation tissue area (D) at the postoperative day 7 harvest date. Data shown as mean $\pm$ SEM.

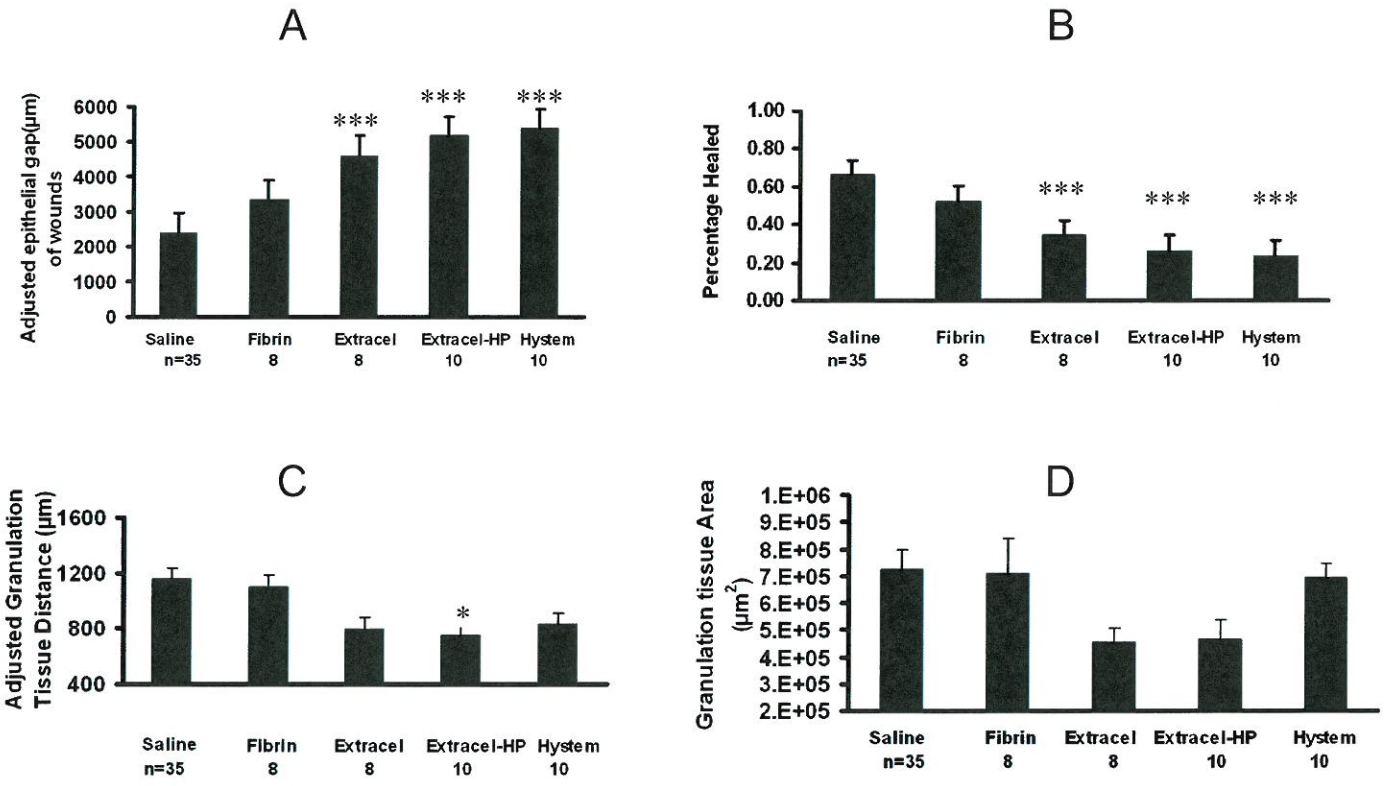

Figure 11. Histological quantification of vehicles treated wounds. Fibrin, Extracel, Extracel-HP, and Hystem treated wounds (7 mm) were compared to saline treated wounds at the postoperative day 7 harvest date. Adjusted epithelial gap (A), percentage healed (B), adjusted granulation tissue distance (C), and granulation tissue area (D) are shown. Data shown as mean $\pm$ SEM. ***$p<0.001$, *$p<0.05$

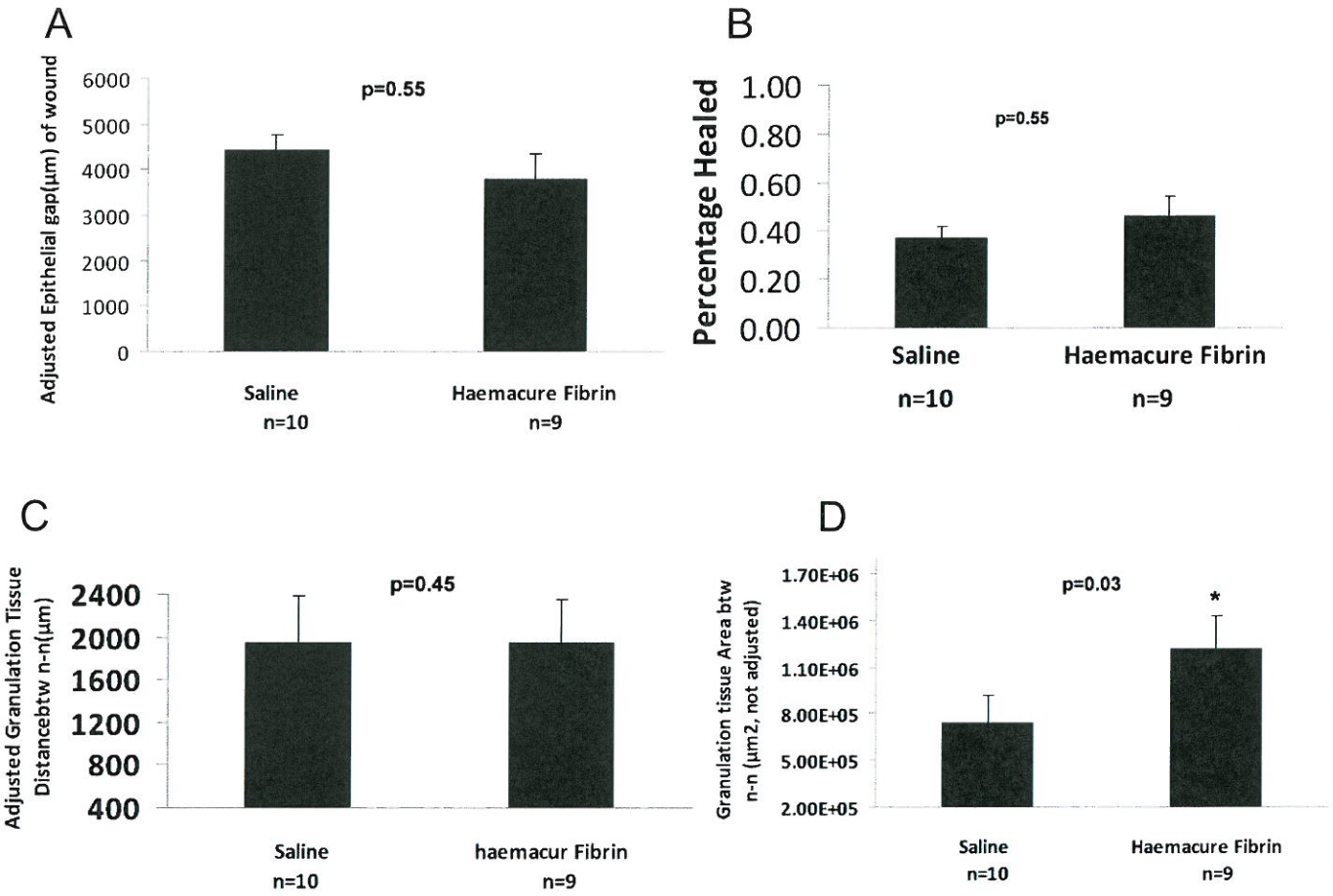

Figure 12. Histological quantification of ASCs treated wounds. ASCs at a concentration of 1 X 10^5 were delivered to 7 mm wounds with Haemacure fibrin or saline. Wounds were harvested at the postoperative day 7 harvest and adjusted epithelial gap (A), percentage healed (B), adjusted granulation tissue distance (C), and granulation tissue area (D) were measure. Data shown as mean $\pm$ SEM. *$p<0.05$

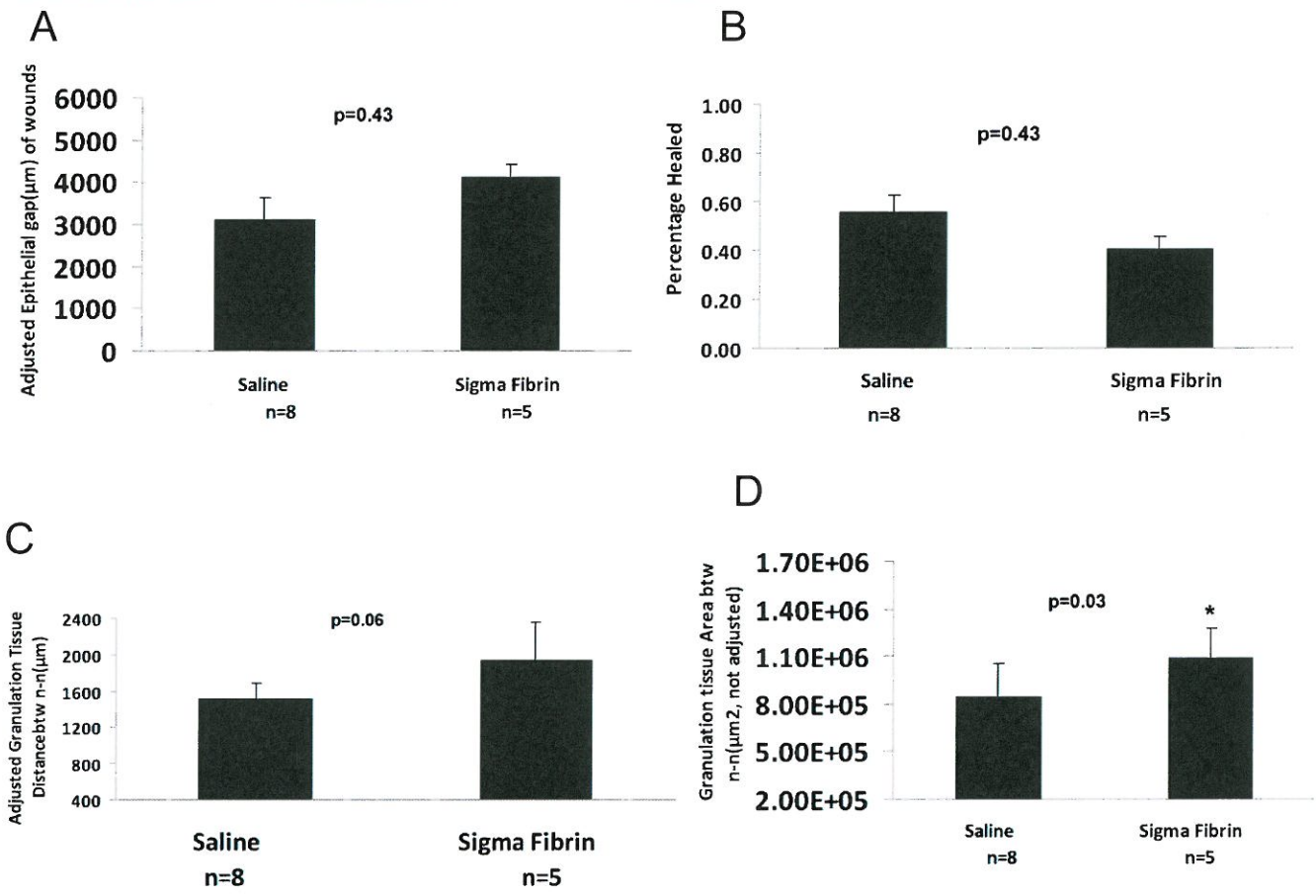

Figure 13. Histological quantification of ASCs treated wounds. ASCs at a concentration of 1 X 10^5 were delivered to 7 mm wounds with Sigma-Aldrich fibrin or saline. Wounds were harvested at the postoperative day 7 harvest and adjusted epithelial gap (A), percentage healed (B), adjusted granulation tissue distance (C), and granulation tissue area (D) were measure. Data shown as mean $\pm$ SEM. *$p<0.05$

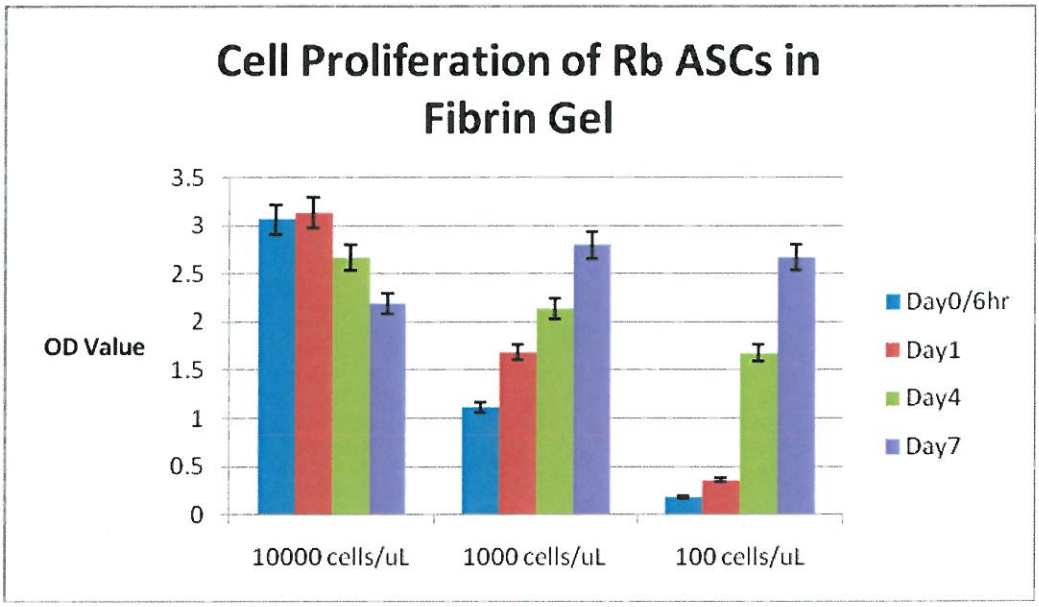

Figure 14. Cell proliferation of rabbit ASCs in fibrin gel over the course of 7 days with three different initial seeding densities (10,000 cells/μL, 1,000 cells/μL, and 100 cells/μL).

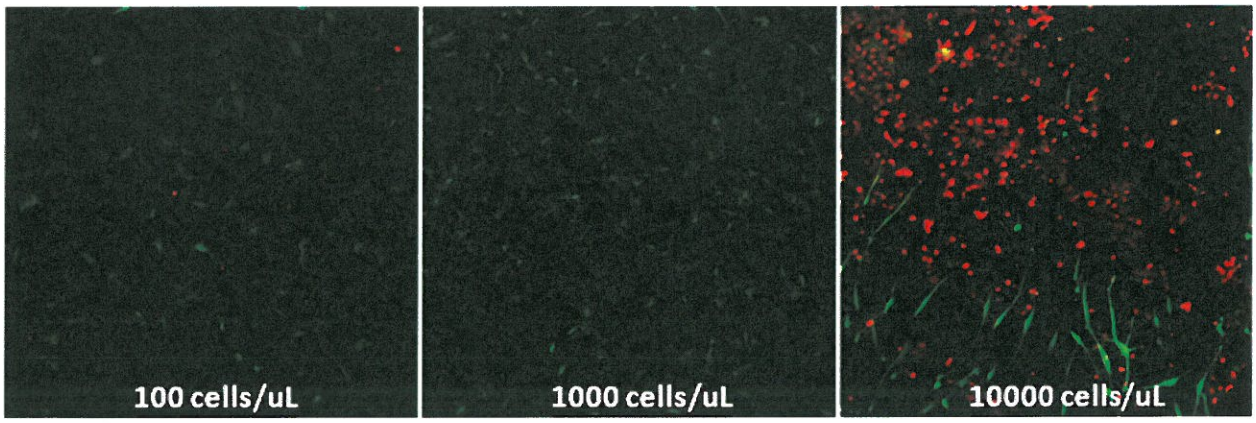

Figure 15. Representative images of live cells (green) and dead cells (red) in fibrin sealant at Day 7 (Zeiss LSM 710; magnification = ×100).

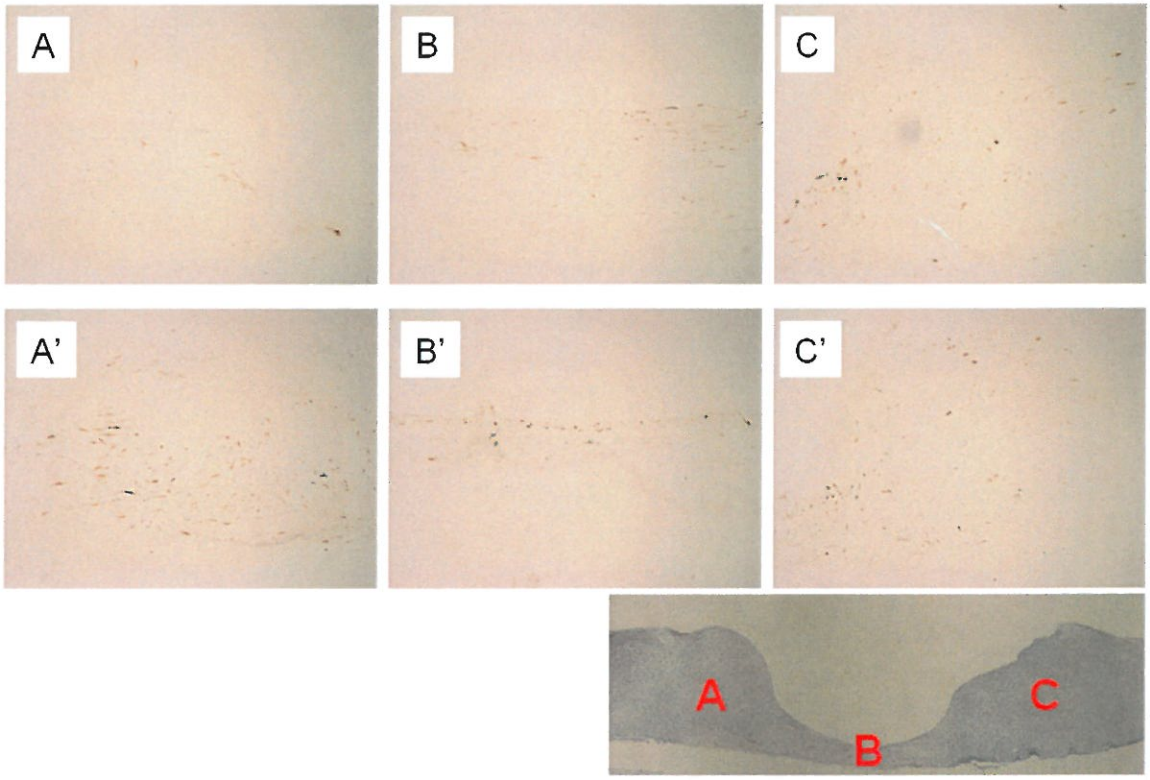

Figure 16. Detection of transplanted ASCs in rabbit ear wounds. GFP expressing ASCs at a concentration of 1 X 10^5 were delivered to 7 mm wounds with saline (A, B, C) or fibrin (A', B', C'). At postoperative day 7 wounds were harvested, expression of GFP was visualized by immunohistochemistry. The analyzed areas were shown in a picture on the bottom which is stained with hematoxylin.

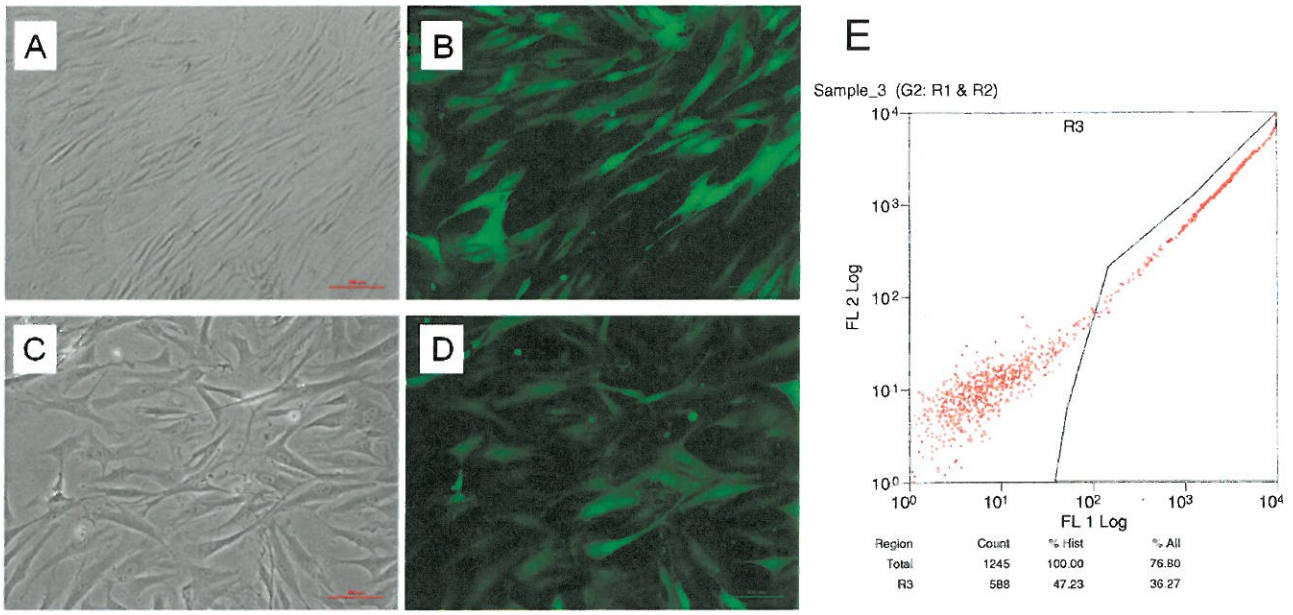

Figure 17. GFP-expressing rabbit ASCs. (A, B) ASCs were transduced with GFP-expressing lentivirus and cultured in the presence of selection marker, blasticidin. GFP negative cells were detected though they are resistant to blasticidin [compare bright image (A) and fluorescence image (B)]. (C, D) Most of the ASCs in bright field (C) showed GFP fluorescence (D) after flow cytometry. (E) An example of flow cytometry is shown. Approximately, 47% of ASCs express GFP before in the population before isolation by flow cytometry

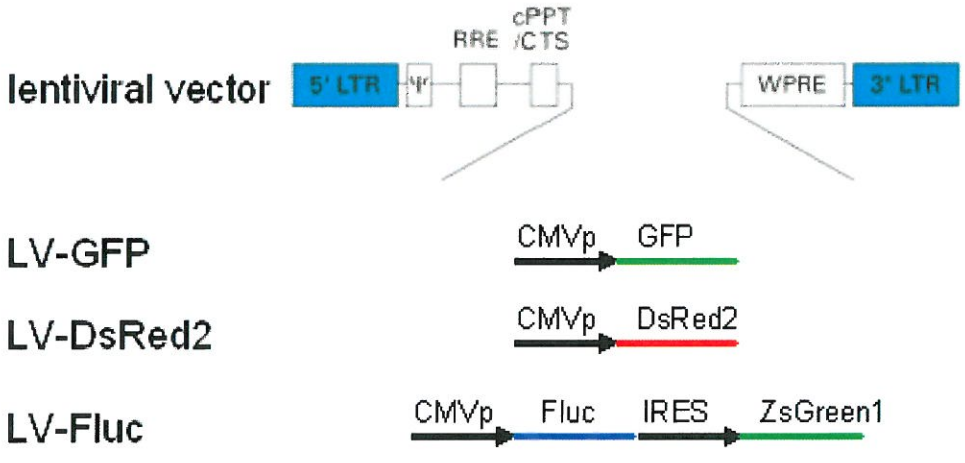

Figure 18. Diagram of lentiviral vectors for the expression of GFP, DsRed2, and Fluc.

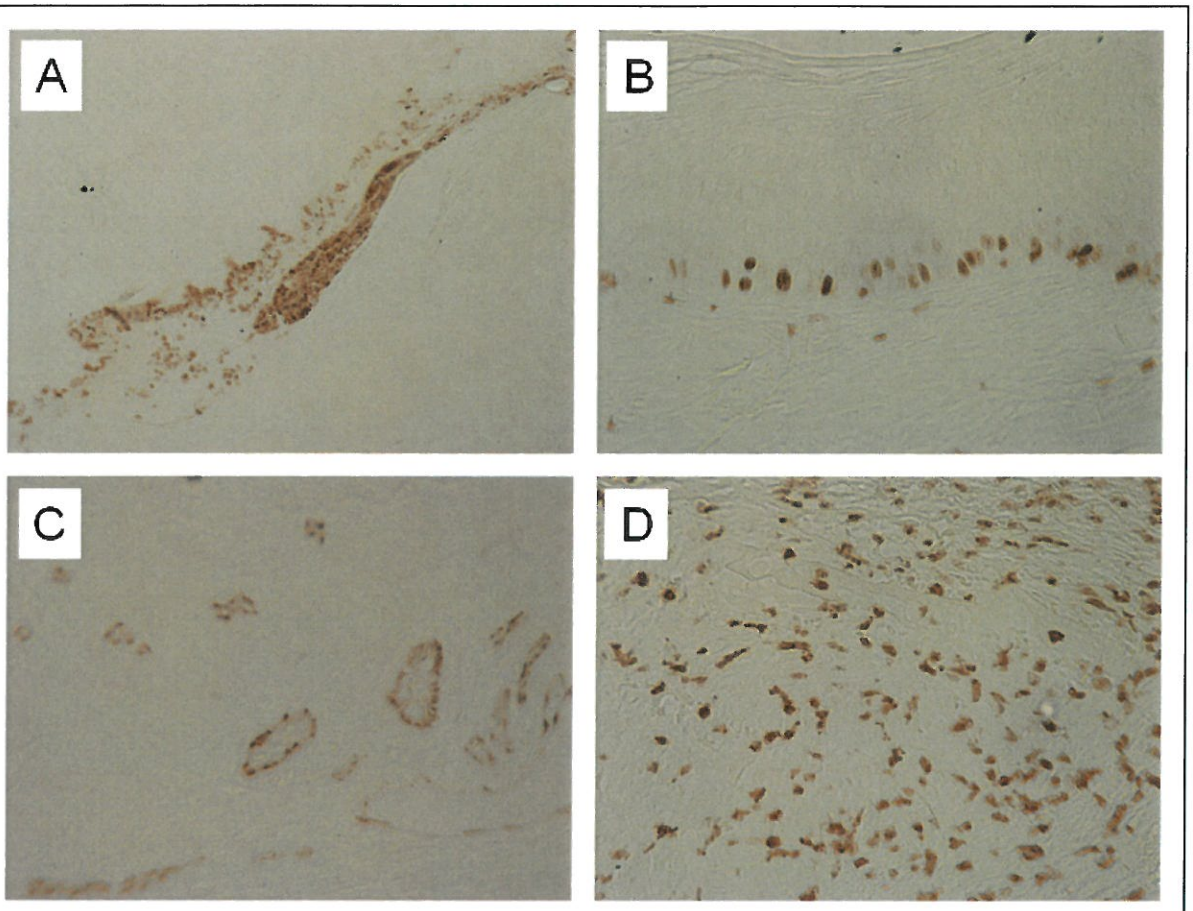

Figure 19. Optimization of immunohistochemitry condition to detect target proteins in rabbit ears. Paraffin embedded tissues were sectioned with 5 μm thickness and processed to incubated antibodies. Anti-neutrophil (A, 1: 1,000 dilution, Santa Cruz Biotechnology), anti-Ki67 (B, 1: 1,000 dilution, BD Biosciences), anti-CD31 (C, 1: 100 dilution, Abcam), and anti-macrophage (D, 1: 1,000 dilution, Abcam) were used as primary antibodies. Signal was visualized by DAB. Magnification A; ×200, B-D; ×400.